Contents lists available at ScienceDirect

Computers and Chemical Engineering

journal homepage: www.elsevier.com/locate/compchemeng

Prediction of the full molecular weight distribution in RAFT polymerization using probability generating functions

Cecilia Fortunatti [1], Claudia Sarmoria [1], Adriana Brandolin [1], Mariano Asteasuain [*]

PLAPIQUI, Camino La Carrindanga km 7, Bahía Blanca 8000, Argentina

A R T I C L E   I N F O

A B S T R A C T

In this work, a model for the RAFT polymerization following the slow fragmentation approach was developed in order to obtain the full molecular weight distribution (MWD) using probability generating functions (pgf). A combination of univariate and bivariate pgf is applied to deal with the univariate chain length distributions of macroradical, dormant and dead polymer chains, and the bivariate distribution of the two arms intermediate adduct. This allows rigorous modeling of the polymerization system without simplifying assumptions. For comparison purposes, the population balances were solved by direct integration of the resulting equations. Our results show that the pgf technique allows obtaining an accurate solution efficiently in terms of computational time. What is more, the model provides a detailed characterization of the polymer that could be of great help for grasp the process fundamentals.

© 2014 Elsevier Ltd. All rights reserved.

1. Introduction

Reversible addition-fragmentation chain-transfer (RAFT) polymerization is recognized as one of the most versatile techniques of controlled radical polymerization (CRP), or reversible-deactivation radical polymerization (RDRP) according to the IUPAC recommendation (Jenkins, Jones, & Moad, 2010). RAFT polymerization is compatible with a wide variety of monomers and requires moderate reaction conditions. Besides, it is effective for the synthesis of block and hyperbranched copolymers. The number of works dealing with the RAFT mechanism and its reported application to the precise synthesis of novel materials evidences the relevance of this polymerization technique (Barner-Kowollik, 2008).

Despite the efforts devoted to understanding the chemistry of this process, there are still unresolved fundamental questions regarding some of the basic steps in the mechanism and kinetics. In this respect, modeling studies are an important tool for aiding in the understanding of this synthesis technique. Several studies have addressed the modeling and simulation of RAFT systems, most of which predict average molecular properties such as average molecular weights and polydispersity. Some of these

works have also included the modeling of the complete MWD. However, rigorous modeling of the MWD in RAFT polymerization requires computing multivariate distributions because of the existence of an intermediate macroradical with two arms. In most of the studies, simplifications have been applied that limit their potential. For instance, adaptations of methods for modeling univariate chain populations have been employed (Wulkow, Busch, Davis, & Barner-Kowollik, 2004). Using this approach it is possible to predict the MWD with respect to the total chain length of the polymer species. However, information is lost about the bidimensional distribution of the two arms of the intermediate adduct that allows knowing how these two arms are interlinked. This knowledge would be useful in the case of specific reactions that take place on just one branch of the intermediate species (Wulkow et al., 2004). Other authors have modeled rigorously the full MWD in RAFT processes by solving the complete set of population balances (Zapata-González, Saldívar-Guerra, & Ortiz-Cisneros, 2011). The drawback of this approach is its high computational cost. The difficulty in model development and execution increases in the case of copolymerization processes and/or prediction of complex molecular architectures.

A particular feature involved in the understanding of RAFT processes is the interpretation of the rate retardation effect. It is well known that the propagation rate in some RAFT polymerization systems is slowed down by increasing the concentration of the chain transfer agent (CTA). However, the cause of this effect has not yet been elucidated definitively from the experimental findings. There are three main lines of thought regarding the

* Corresponding author. Tel.: +54 291 4861700; fax: +54 291 4861600.
E-mail addresses: cfortunatti@plapiqui.edu.ar (C. Fortunatti), csarmoria@plapiqui.edu.ar (C. Sarmoria), abrandolin@plapiqui.edu.ar (A. Brandolin), masteasuain@plapiqui.edu.ar (M. Asteasuain).
[1] Tel.: +54 291 4861700.

mechanism and kinetics of the RAFT reactions in order to explain this characteristic rate retardation effect:

Slow Fragmentation (SF) Model: Barner-Kowollik, Quinn, Nguyen, Heuts, and Davis (2001) proposed that this retardation is due to the slow fragmentation of the two arms adduct (small fragmentation constant k_f). This leads to a large equilibrium constant ($K = k_a/k_f$) consistent with experiments, but it predicts radical concentrations that are lower and intermediate adduct concentrations that are higher than experimental findings.

Intermediate Radical Termination (IRT) Model: Monteiro and De Brouwer (2001) attributed the rate retardation to the cross-termination of the adduct radicals with propagating radicals, which could explain the three arms polymers that have been detected experimentally. In addition, the radical concentration predicted by this model is consistent with data. However, the concentration of the three arms polymer predicted by this theory is higher than experimental observations.
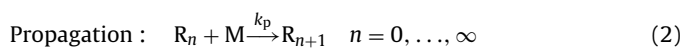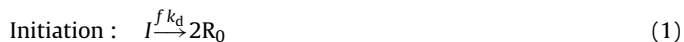
Intermediate Radical Termination with Oligomers (IRTO) Model: this model could be considered a combination of the previous two (Konkolewicz, Hawkett, Gray-Weale, & Perrier, 2008). In an attempt to reconcile the experimental findings with the theory, this model proposes that adduct radicals cross-terminate but only with oligomeric propagating radicals up to two monomers long. The value of the equilibrium constant and the intermediate adduct concentration calculated with this model are in agreement with those estimated by *ab initio* calculations and experimental electron spin resonance (ESR) studies, respectively (Zapata-González et al., 2011).

In this work, a mathematical model of a SF interpretation of the RAFT polymerization, capable of predicting the full MWD of the polymer as well as average molecular properties, is developed. Its extension to the IRT or IRTO model is straightforward and will be developed in future works. The model provides detailed information on the molecular structure of the polymer that is very useful for gaining insight in the process fundamentals and for the process operation.
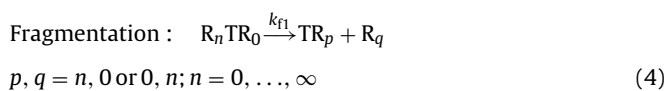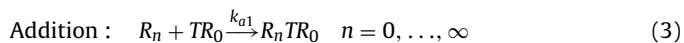
2. Methods

2.1. Kinetic mechanism

CRP is based on establishing equilibriums between active and inactive chains. The interactions between living chains are limited by the addition of an agent that can deactivate them reversibly. In the RAFT processes it is achieved by introducing an intermediate species with symmetrical structure that can release a radical from either end and continue the propagation of monomers (Zhang & Ray, 2001). The kinetic mechanism for the RAFT reaction according to the SF model is as follows:

Initiation : $\quad I \xrightarrow{f\,k_d} 2R_0$ (1)

Propagation : $\quad R_n + M \xrightarrow{k_p} R_{n+1} \quad n = 0, \ldots, \infty$ (2)

Pre equilibrium

Addition : $\quad R_n + TR_0 \xrightarrow{k_{a1}} R_n TR_0 \quad n = 0, \ldots, \infty$ (3)

Fragmentation : $\quad R_n TR_0 \xrightarrow{k_{f1}} TR_p + R_q$

$p, q = n, 0 \text{ or } 0, n; n = 0, \ldots, \infty$ (4)

Core equilibrium

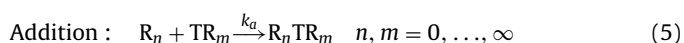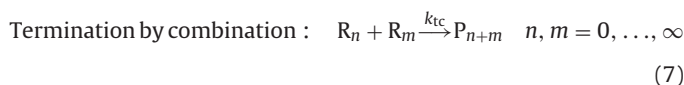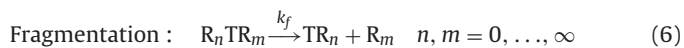Addition : $\quad R_n + TR_m \xrightarrow{k_a} R_n TR_m \quad n, m = 0, \ldots, \infty$ (5)

Table 1
Kinetic parameters (Zapata-González et al., 2011).

Reaction	Parameter	Units
Initiation	$f = 0.5$	
	$k_d = 0.036$	h^{-1}
Propagation	$k_p = 3.6 \times 10^6$	$\text{L mol}^{-1}\,\text{h}^{-1}$
Addition	$k_a = 3.6 \times 10^9$	$\text{L mol}^{-1}\,\text{h}^{-1}$
Fragmentation	$k_f = 36$	h^{-1}
Termination by combination	$k_{tc} = 3.6 \times 10^{10}$	$\text{L mol}^{-1}\,\text{h}^{-1}$
Termination by disproportionation	$k_{td} = 3.6 \times 10^{10}$	$\text{L mol}^{-1}\,\text{h}^{-1}$

Fragmentation : $\quad R_n TR_m \xrightarrow{k_f} TR_n + R_m \quad n, m = 0, \ldots, \infty$ (6)

Termination by combination : $\quad R_n + R_m \xrightarrow{k_{tc}} P_{n+m} \quad n, m = 0, \ldots, \infty$ (7)

Termination by disproportionation :

$\quad R_n + R_m \xrightarrow{k_{td}} P_n + P_m \quad n, m = 0, \ldots, \infty$ (8)
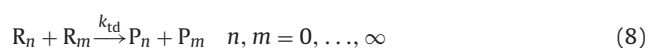
The chemical species involved are: initiator (I), monomer (M), active radicals with n units of M (R_n), dormant (inactive) radicals with n units of M (TR_n), intermediate (adduct) radicals with two arms of different length ($R_n TR_m$), and terminated (dead) polymer chains of length n (P_n). The chain transfer agent is regarded as an inactive radical with 0 units of monomer (TR_0). For simplicity, a single set of constants was used for both the pre-equilibrium and the core equilibrium ($k_{a1} = k_a$, $k_{f1} = k_f$). Nevertheless, applying the methodology using different sets of constants for the two equilibriums would be straightforward.

Table 1 shows the set of kinetic parameters that was used in this work. These are typical parameters for a methyl methacrylate homopolymerization. It is worth noting that the cross-termination reaction between the intermediate adduct and propagating radicals is not considered and that the value of k_f is relatively low, in agreement with the SF theory.

The two arms adduct contributes significantly to the overall polymer MWD because of its high proportion in the chain population. Therefore, the accurate description of the concentration of this species is of fundamental importance. This involves dealing with a bivariate distribution of chain length, because the sizes of the two arms of this adduct are independent of each other.

2.2. Mathematical modeling

2.2.1. Average properties
The model development is based on the population balances drawn from the kinetic mechanism. The well-known method of moments is used to transform these balances for modeling average molecular properties. The moments involved in the mathematical model are defined below:

Moment of order "a" of living radicals

$$\lambda_a \sum_{n=0}^{\infty} n^a [R_n]$$ (9)

Moment of order "a" of dormant radicals

$$\mu_a^I = \sum_{n=0}^{\infty} n^a [TR_n]$$ (10)

Moment of order "a,b" of adduct radicals

$$\mu_{a,b}^{II} \sum_{n=0}^{\infty} \sum_{s=0}^{\infty} n^a s^b [R_n TR_s]$$ (11)

Moment of order "a" of adduct radicals considering their total length

$$\mu_a^{II} = \sum_{n=0}^{\infty} n^a [RTR_n] \tag{12}$$

where RTR_n is a two arms adduct of total length n

Partial moment of order 0 of adduct radicals

$$d\mu_{0\ n}^{II} = \sum_{s=0}^{\infty} [R_n TR_s] \tag{13}$$

The population balances resulting from the kinetic mechanism are:

Initiator

$$\frac{d}{dt}([I]) = -k_d[I] \tag{14}$$

Monomer

$$\frac{d}{dt}([M]) = -k_p[M]\lambda_0 \tag{15}$$

Active radicals with n units of monomer (R_n)

$$\frac{d}{dt}([R_n]) = 2f\,k_d[I]\delta_{n,0} + k_p[M][R_{n-1}](1-\delta_{n,0}) + (1/2)k_f d\mu_{0\ n}^{II}$$
$$- (k_p[M] + k_a\mu_0^I + (k_{tc}+k_{td})\lambda_0)[R_n] \tag{16}$$

Dormant radicals with n units of monomer (TR_n)

$$\frac{d}{dt}([TR_n]) = -k_a\lambda_0[R_n] + (1/2)k_f d\mu_{0\ n}^{II} \tag{17}$$

Adduct radicals with two arms of length n and m ($R_n TR_m$)

$$\frac{d}{dt}([R_n TR_m]) = -k_f[R_n TR_m] + k_a([R_n][TR_m] + [R_m][TR_n]) \tag{18}$$

Partial moment of order 0 of adduct radicals:

$$\frac{d}{dt}(d\mu_{0\ n}^{II}) = -k_f d\mu_{0\ n}^{II} + k_a(\lambda_0[TR_n] + \mu_0^I[R_n]) \tag{19}$$

Dead polymer chains of length n (P_n):

$$\frac{d}{dt}([P_n]) = k_{td}\lambda_0[R_n] + (1/2)k_{tc}\sum_{i=0}^{n} ([R_{n-1}][R_i]) \tag{20}$$

Applying the method of moments to the mass balances of the polymeric species, the following moment equations are obtained:

Moment of order "a" of active radicals (λ_a), a = 0,1,2

$$\frac{d}{dt}(\lambda_a) = 2f\,k_d[I](0)^a + k_p[M]\sum_{j=0}^{a}\binom{a}{j}\lambda_j + (1/2)\,k_f\mu_a^{II}$$
$$- \left(k_p[M] + k_a\mu_0^I + (k_{tc}+k_{td})\lambda_0\right)\lambda_a \tag{21}$$

Moment of order "a" of dormant radicals (μ_a^I), a = 0,1,2

$$\frac{d}{dt}(\mu_a^I) = k_a\lambda_0\mu_a^I + (1/2)k_f\mu_a^{II} \tag{22}$$

Moment of order "a,b" of adduct radicals ($\mu_{a,b}^{II}$), a,b = 0,1,2

$$\frac{d}{dt}\left(\mu_{a,b}^{II}\right) = -k_f\mu_{a,b}^{II} + k_a\left(\lambda_a\mu_b^I + \lambda_b\mu_a^I\right) \tag{23}$$

Moment of order "a" of adduct radicals considering their total length (μ_a^{II}), a = 0,1,2

$$\frac{d}{dt}\left(\mu_a^{II}\right) = -k_f\mu_a^{II} + k_a\sum_{j=0}^{a}\binom{a}{j}\lambda_{a-j}\mu_j^I \tag{24}$$

This moment can also be calculated as :

$$\mu_a^{II} = (1/2)\sum_{j=0}^{a}\binom{a}{j}\mu_{a-j,j}^{II} \tag{25}$$

Moment of order "a" of dead polymer chains (ε_a), a = 0,1,2

$$\frac{d}{dt}(\varepsilon_a) = k_{td}\lambda_0\lambda_a + (1/2)k_{tc}\sum_{j=0}^{a}\binom{a}{j}\lambda_{a-j}\lambda_j \tag{26}$$

The number $\bar{M}_n$ and weight $\bar{M}_w$ average molecular weights are computed from the MWD moments according to:

$$\bar{M}_n = M_{w,M}\frac{\lambda_1 + \mu_1^I + \mu_1^{II} + \varepsilon_1}{\lambda_0 + (\mu_0^I - TR_0) + (\mu_0^{II} - R_0 TR_0) + \varepsilon_0} \tag{27}$$

$$\bar{M}_w = M_{w,M}\frac{\lambda_2 + \mu_2^I + \mu_2^{II} + \varepsilon_2}{\lambda_1 + \mu_1^I + \mu_1^{II} + \varepsilon_1} \tag{28}$$

where $M_{w,M}$ is the molecular weight of the monomer.

2.3. Full MWD

The probability generating function (pgf) technique is employed to model the full MWD of the polymer. This technique consists in transforming the mass balances of polymeric species, characterized by the number of units of monomer, to the pgf domain. As a result, balances for the pgf transform of the MWD are obtained. After solving the pgf balances, the full MWD is recovered from the pgf domain by applying an appropriate inversion method. It is important to point out that this method does not require any a priori knowledge of the MWD shape and is able to deal with complex kinetic mechanisms.

A combination of unimodal (Asteasuain, Sarmoria, & Brandolin, 2002; Sarmoria, Asteasuain, & Brandolin, 2012) and bimodal (Asteasuain & Brandolin, 2010) pgfs are applied to the population balances to model the MWD of the different polymeric species.

The univariate pgf of order a ($\vartheta_a = \phi_a, \varphi_a, \psi_a, \chi_a$) of any species X_n ($X_n = R_n, TR_n, P_n$) is defined as follows:

$$\vartheta_a(z) = \sum_{n=0}^{\infty} z^n n^a \frac{[X_n]}{\delta_n} \tag{29}$$

where δ_a is the moment of order a of species X_n ($\delta_a = \lambda_a, \mu_a^I, \mu_a^{II}, \varepsilon_a$). The bivariate pgf of order a,b ($\psi_{a,b}$) of species $R_n TR_m$ with one arm of length n and another one of length m is defined as follows:

$$\psi_{a,b}(z,w) = \sum_{n=0}^{\infty} z^n n^a \sum_{m=0}^{\infty} w^m m^b \frac{[R_n TR_m]}{\mu_{a,b}^{II}} \tag{30}$$

where $\mu_{a,b}^{II}$ is the double index moment of order a, b of species $R_n TR_m$, while z and w are the dummy variables of the pgf. Applying the pgf transformation to the mass balances of the polymeric species (Eqs. (15)–(17) and (19)) as described in Asteasuain, Sarmoria, and Brandolin (2002), Sarmoria et al. (2012) and Brandolin and Asteasuain (2013), the following pgf balances are obtained:

pgf of order 0 of living radicals ($\phi_0(z)$):

$$\frac{d}{dt}(\lambda_0\phi_0(z)) = 2fk_d[I] + k_p[M][z(l_0\phi_0(z)) - (\lambda_0\phi_0(z))]$$
$$- k_a\mu_0(\lambda_0\phi_0(z)) + (1/2)k_f\left(\mu_0^{II}\psi_{0,0}(z,1)\right)$$
$$- (k_{tc}+k_{td})\lambda_0(\lambda_0\phi_0(z)) \tag{31}$$

pgf of order 0 of dormant radicals ($\varphi_0(z)$):

$$\frac{d}{dt}(\mu_0^I \varphi_0(z)) = -k_a \lambda_0 (\mu_0^I \varphi_0(z)) + (1/2)k_f (\mu_{0,0}^{II} \psi_{0,0}(z,1)) \qquad (32)$$

Univariate pgf of order 0 of adduct radicals ($\psi_0(z)$):

$$\frac{d}{dt}\left(\mu_0^{II}\psi_0(z)\right) = k_a \left(\lambda_0 \phi_0(z)\right)\left(\mu_0^I \varphi_0(z)\right) - k_f \left(\mu_0^{II}\psi_0(z)\right) \qquad (33)$$

Bivariate pgf of order 0,0 of adduct radicals ($\psi_{0,0}(z,w)$) evaluated at $w = 1$:

$$\frac{d}{dt}\left(\mu_{0,0}^{II}\psi_{0,0}(z,1)\right) = k_a \mu_0 \left(\lambda_0 \phi_0(z)\right) + k_a \lambda_0 \left(\mu_0^I \varphi_0(z)\right)$$
$$- k_f \left(\mu_{0,0}^{II}\psi_{0,0}(z,1)\right) \qquad (34)$$

pgf of order 0 of dead polymer chains ($\chi_0(z)$):

$$\frac{d}{dt}(\varepsilon_0 \chi_0(z)) = k_{td}\lambda_0 \left(\lambda_0 \phi_0(z)\right) + (1/2)\,k_{tc}(\lambda_0 \phi_0(z))^2 \qquad (35)$$

pgf of order 0 of the overall polymer $R_n + TR_n + RTR_n + P_n$ ($\Omega_0(z)$):

$$\Omega_0(z) = \frac{\lambda_0 \phi_0(z) + \mu_0^I \varphi_0(z) + \mu_0^{II}\psi_0(z) + \varepsilon_0 \chi_0(z)}{\lambda_0 + \mu_0^I + \mu_0^{II} + \varepsilon_0} \qquad (36)$$

This system couples univariate and bivariate pgfs of the distributions of the different polymer species. It should be noted that the products of the pgfs by the corresponding moments are treated as dependent variables in the pgf balances (e.g. ($\varepsilon_0 \chi_0(z)$) in the pgf balance of $\chi_0(z)$). This results in more compact equations and avoids indeterminations in the initial conditions when the concentration of the species is zero. Pgf values are extracted from the product of the pgf and the moment by solving the moment equations independently.

Once the pgf balances are solved the pgf are numerically inverted using an appropriate inversion method (Asteasuain, Brandolin, & Sarmoria, 2002; Sarmoria et al., 2012; Brandolin & Asteasuain, 2013). Only pgfs of order 0 are computed, which yields the MWD expressed in number fraction (Asteasuain, Sarmoria, & Brandolin, 2002). The weight fraction distribution is obtained by operating with the number fraction distribution. The inversion method requires the user to specify a parameter N that affects the calculation of the MWD and the size of the system of equations. The user should set an appropriate value of N, large enough to avoid poor accuracy and low enough to avoid introducing numerical noise (Sarmoria et al., 2012). In this work, the full MWD of the overall polymer is reported, which is recovered by inverting $\Omega_0(z)$ without the need of any simplifying assumptions or hypotheses. In addition, the model consists of a relatively small number of equations that can be solved in a reasonable time.

All the simulations were performed in gPROMS (Process Systems Enterprise, Ltd.) in a standard desktop computer. This software provides a range of state-of-the-art proprietary solvers for the execution of different types of activities, such as simulation or optimization. In this work the solver DASOLV was used for the model simulation. DASOLV is a standard solver for mixed sets of differential and algebraic equations, based on variable time step/variable order Backward Differentiation Formulae (BDF). This solver is designed to deal with large, sparse systems of equations in which the variable values are restricted to lie within specified lower and upper bounds.

3. Results and discussion

A RAFT polymerization system was simulated following the SF interpretation of the process. The model was solved both by direct integration of the population balances and using the pfg technique, in order to evaluate the efficiency and reliability of the latter. To

Table 2
Common conditions for simulations at fixed final reaction time.

Condition	Value	Units
$[M]_0$	5	mol L^{-1}
$[CTA]_0$	1×10^{-2}	mol L^{-1}
Final reaction time	34	h

perform this comparison, several runs were carried out for different initial concentrations of CTA and initiator, in order to obtain polymers with different molecular weights and MWDs.

3.1. Fixed final reaction time

To begin with the comparison, three runs with different initial concentration of initiator were performed while final reaction time and the initial concentration of CTA were kept at a fixed value. The common parameters for the simulations are shown in Table 2.

Simulation results at final reaction time are presented in Fig. 1. The complete MWD of the polymer, as well as the number average molecular weight, polydispersity index (PDI) and the fraction of dormant radicals are included. The amount of inactive radicals is also presented. This quantity is especially important for any CRP because those species are able to further polymerize and its concentration determines how uniformly polymer chains can grow.

It can be observed that the points obtained with the pgf technique closely follow the MWD shape obtained by direct integration of mass balances. Consequently, the pgf technique can be considered as a reliable method to model this polymerization process.

It is important to mention that independent subsets of model equations are solved for computing each point of the MWD when using the pfg technique. Thus, the MWD can be drawn as smoothly as desired by changing the number of points to be computed. In the same way, the size of the resulting differential algebraic equation (DAE) system could be reduced if fewer points were enough.

It should be stressed that, for this set of kinetic parameters, the MWDs show a marked bimodality. The higher molecular weight peak corresponds to the population of the two arms adduct, and the other one to the remaining species. The SF theory predicts a significant concentration of the two arms adduct, enough for generating distinguishable peak in the MWD. This observation has been previously reported in the literature, and has been suggested as potential means of discrimination between the theoretical interpretations of the RAFT mechanism (Zapata-González et al., 2011). It may also be seen that the high molecular weight peak corresponds to a chain length twice as large as the one corresponding to the other peak in all simulations. This is expected since the intermediate adduct is the result of the union of two chains from a population of chains of approximately equal size. As the reaction proceeds (i.e. greater conversion), the concentration of the adduct increases at the expense of the other species, so that the adduct peak becomes higher and the other one becomes lower.

It is worth noting that average molecular properties provide insufficient information to properly characterize the produced resins, since it is not possible to determine whether the polymer MWD is bimodal from the average properties only.

It can be seen that by increasing the initial concentration of initiator, polymers of higher molecular weights are obtained. This behavior, opposite to what happens in conventional radical polymerizations, is due to the living features of the RAFT process. In RAFT polymerization, as long as there is no significant bimolecular termination, nearly all polymer chains are living chains in their dormant state. Furthermore, the number of chains is approximately constant and equal to the initial concentration of transfer agent. Therefore,

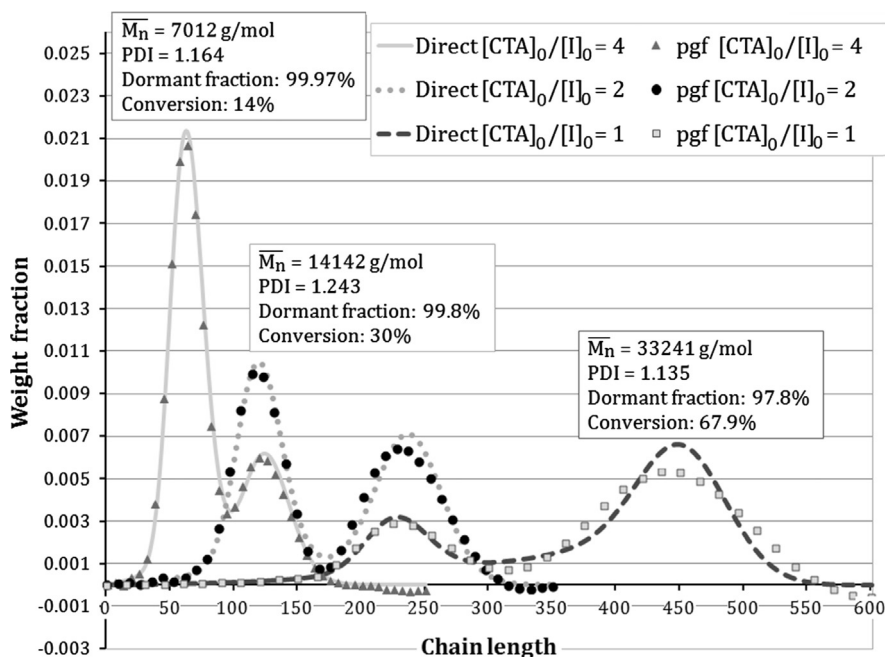$$\bar{M}_n \approx \frac{M_{w,M} Conv [M]_0}{[CTA]_0} \qquad (37)$$

Fig. 1. Full MWD of polymers obtained with $[CTA]_0 = 1 \times 10^{-2}$ mol L^{-1} and different $[I]_0$.

This means that for a given conversion of monomer, $\bar{M}_n$ depends only on the initial concentration of transfer agent. On the other hand, increasing initiator concentration accelerates the polymerization rate, causing higher conversions to be achieved in the same time. Simulation outcomes allow verifying that the approximate expression given by Tobita (2010) for the polymerization rate matches the actual rate:

$$Rp = k_p \ [M] \ \lambda_0 \ (actual) \approx k_p \ [M] \ \frac{k_f}{k_a} \ \frac{\mu_0^{II}}{\mu_0^{I}} (Tobita) \qquad (38)$$

When increasing the initiator concentration, and hence the source of free radicals, the equilibrium reaction

$$R_n + TR_m \underset{k_f}{\overset{k_a}{\rightleftharpoons}} R_n TR_m \qquad (39)$$

is shifted to the right, and consequently, the polymerization rate augments according to Eq. (38). However, due to the living character of the polymerization process, the total number of chains is practically unchanged. Hence, as can be seen in Fig. 2 the dependency of $\bar{M}_n$ with conversion does not vary for any of the studied cases because the initial transfer agent concentration is the same. Nevertheless, the reaction proceeds faster when the initial initiator
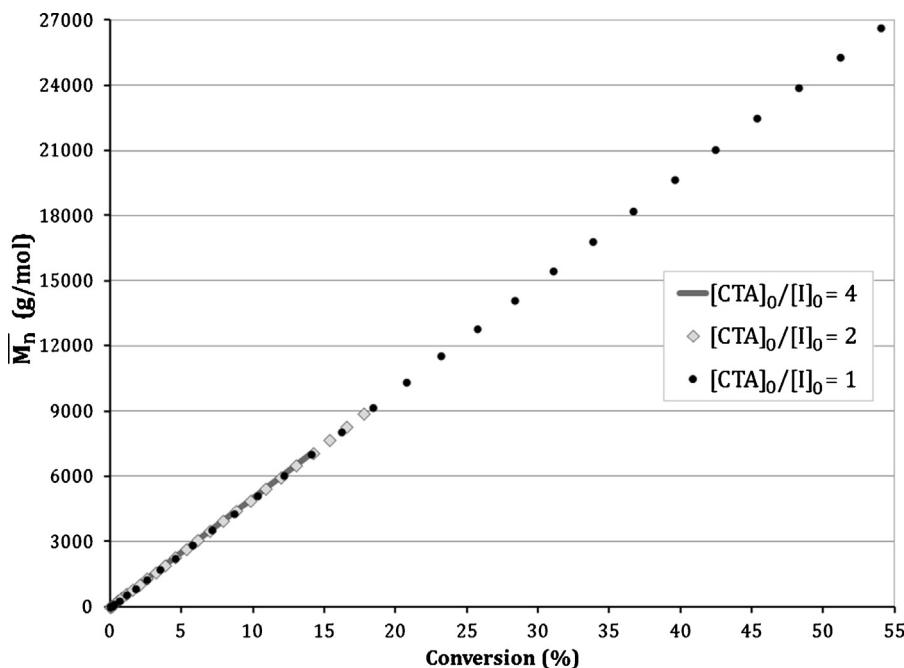

Fig. 2. $\bar{M}_n$ vs. conversion for different $[I]_0$ and $[CTA]_0 = 1 \times 10^{-2}$ mol L^{-1}.

Table 3
Common conditions for simulations at fixed final monomer conversion.

Condition	Value	Units
$[M]_0$	5	$mol\,L^{-1}$
$[I]_0$	5×10^{-3}	$mol\,L^{-1}$
Final monomer conversion	30%	–

Table 4
Efficiency variables for both resolution methods.

Fixed Condition	$[CTA]_0/[I]_0$	Max. chain length	Method	CPU time (s)
$[CTA]_0 = 1 \times 10^{-2}$	4	250	**pgf**	6
			Direct	10
$[CTA]_0 = 1 \times 10^{-2}$	2	350	**pgf**	6
			Direct	20
$[I]_0 = 5 \times 10^{-3}$	2	500	**pgf**	5
			Direct	36
$[CTA]_0 = 1 \times 10^{-2}$	1	600	**pgf**	6
			Direct	56
$[I]_0 = 5 \times 10^{-3}$	1	800	**pgf**	6
			Direct	88
$[I]_0 = 5 \times 10^{-3}$	0.5	1100	**pgf**	6
			Direct	159
$[I]_0 = 5 \times 10^{-3}$	0.25	1850	**pgf**	6
			Direct	408

concentration is increased and higher $\bar{M}_n$ can be obtained for the same reation time.

3.2. Fixed final monomer conversion

Another four runs were performed with the same initial concentration of initiator and final monomer conversion. The initial concentration of CTA was changed to evaluate variations in polymer properties. The common parameters for these simulations are shown in Table 3.

Fig. 3 shows the MWD of the obtained polymers for each simulation. The $\bar{M}_n$, PDI and final reaction time are also presented in the figure. Again, it can be seen that the MWDs are bimodal. Besides, the $\bar{M}_n$ increases as $[CTA]_0$ diminishes for the given monomer conversion, as Eq. (37) predicts.

It is also possible to observe that reaction rate increases for lower $[CTA]_0$, since shorter reaction times are needed for achieving the fixed conversion of 30%. This again agrees with Eq. (38), which predicts higher polymerization rate for lower concentration of dormant radicals ($\mu_0^I \approx [CTA]_0$). It is important to remark that the results presented for this case and for the previous ones, indicate two different operating options for controlling polymerization rate and molecular weight. On one hand, changing initiator concentration allows modifying the polymerization rate with no effect on the $\bar{M}_n$ vs. conversion slope. On the other, varying the initial transfer agent concentration has the effect of changing the polymerization rate and the $\bar{M}_n$ vs. conversion slope in the same direction: decreasing initial transfer agent concentration increases both the polymerization rate and the slope of the $\bar{M}_n$ vs. conversion curve. The latter behavior is shown in Fig. 4. It can also be observed in this figure that the calculated $\bar{M}_n$ profile matches the approximate expression in Eq. (37) in most cases. The approxima-

tion is good only as long as the initial concentration of CTA is large enough to keep the amount of terminated chains ("dead" polymer) negligible. When $[CTA]_0$ diminishes, the equilibrium shown in Eq. (39) shifts to the left, causing an increase in the active radicals concentration and hence of bimolecular termination. Therefore, the total population of polymer chains is no longer (nearly) equal to the number of pseudoliving chains and the $\bar{M}_n$ does not behave according to Eq. (37).

3.3. Efficiency of pgf technique

To evaluate the efficiency of the method in terms of computational effort, the required computation time is shown in Table 4. In all cases, the DAE system resulted from the pgf technique could be solved faster than the direct integration of mass balances.

The number of population balances to be solved by direct integration strongly depends on the molecular weight range of the physical system, because a balance equation needs to be solved for each chain up to the maximum significant length defined by the user. In contrast, the size of the DAE system that results from the pgf method only depends on the value of parameter N and on the number of points that are being recovered. Given that, the simulation
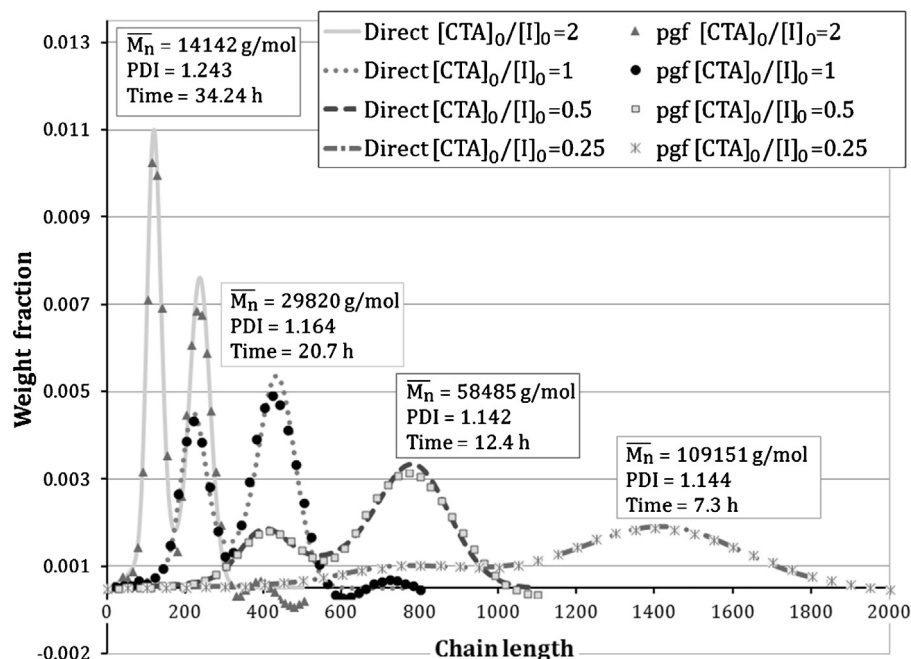

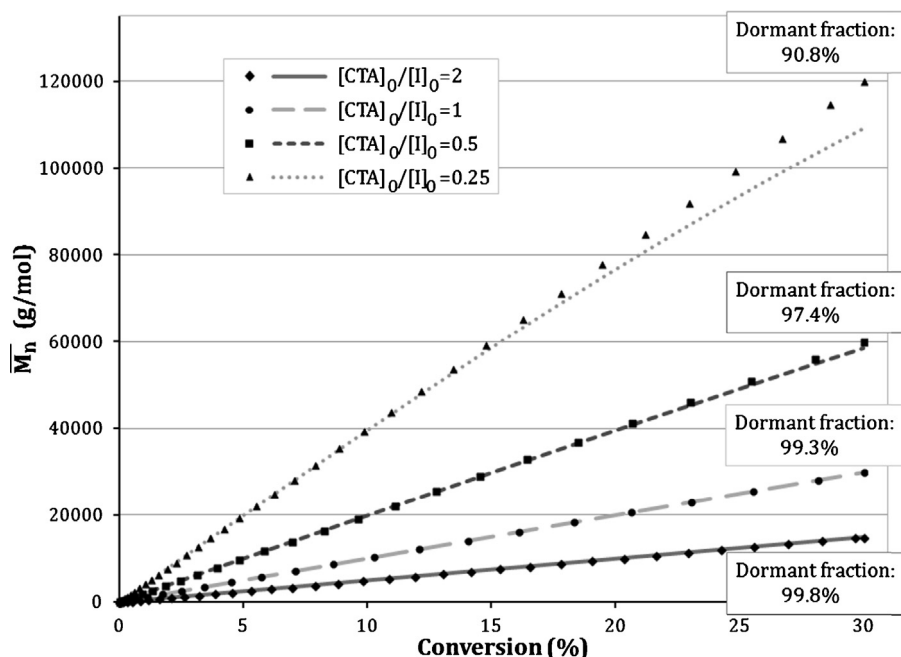**Fig. 3.** Full MWD of polymers obtained with different $[CTA]_0$.

Fig. 4. $\bar{M}_n$ vs. conversion for different $[CTA]_0$ and $[I]_0 = 5 \times 10^{-3}$ mol L^{-1}. Symbols: approximate $\bar{M}_n$ calculated with Eq. (37); lines: SF model.

time required to obtain the MWD through the pgf technique does not change regardless of the molecular weight while it increases considerably for the direct integration solution. The small difference in the time for simulations using the pgf technique shown in Table 4 is due to changes in the value of parameter N of the pgf inversion method.

4. Conclusions

The RAFT polymerization with the slow fragmentation model kinetics has been successfully modeled using the pgf technique. The model allows obtaining the full MWD fast and accurately, with small demands of computational resources.

The combination of univariate and bivariate pgf allows computing the polymer MWD, in spite of the bivariate nature of the MWD of the intermediate adduct, without any simplifying assumptions or MWD shape assumptions. Moreover, the model size is independent of the significant chain length range of the polymer system. Two different operating options for controlling polymerization rate and molecular weight were presented. By increasing the initial initiator concentration the reaction proceeds faster and allows the obtainment of polymers with higher molecular weights for the same reaction time. However, the dependence of the number average molecular weight with conversion remains unchanged. On the other hand, when a higher initial amount of chain transfer agent is fed the rate of polymerization decreases and lower $\bar{M}_n$ resins are obtained for the same monomer conversion.

These results show that the pgf technique can provide detailed information on the polymer molecular structure and process fundamentals and that it has great potential to shed light on some essential issues of RAFT processes kinetics.

Acknowledgements

References

Asteasuain, M., Sarmoria, C., & Brandolin, A. (2002). Recovery of molecular weight distributions from transformed domains. Part I. Application of pgf to mass balances describing reactions involving free radicals. *Polymer, 43,* 2513–2527.

Asteasuain, M., Brandolin, A., & Sarmoria, C. (2002). Recovery of molecular weight distributions from transformed domains. Part II. Application of numerical inversion methods. *Polymer, 43,* 2529–2541.

Asteasuain, M., & Brandolin, A. (2010). Mathematical modeling of bivariate polymer property distributions using 2D probability generating functions, 1 – Numerical inversion methods. *Macromolecular Theory and Simulations, 19,* 342–359.

Barner-Kowollik, C. (2008). *Handbook of RAFT Polymerization.* Weinheim, Germany: Wiley-VCH.

Barner-Kowollik, C., Quinn, J. F., Nguyen, T. L. U., Heuts, J. P. A., & Davis, T. P. (2001). Kinetic investigations of reversible addition fragmentation chain transfer polymerizations: Cumyl phenyldithioacetate mediated homopolymerizations of styrene and methyl methacrylate. *Macromolecules, 34,* 7849–7857.

Brandolin, A., & Asteasuain, M. (2013). Mathematical modeling of bivariate distributions of polymer properties using 2D probability generating functions. Part II. Transformation of population mass balances of polymer processes. *Macromolecular Theory and Simulations, 22,* 273–308.

Jenkins, A. D., Jones, R. G., & Moad, G. (2010). Terminology for reversible-deactivation radical polymerization previously called "controlled" radical or "living" radical polymerization (IUPAC recommendations 2010). *Pure and Applied Chemistry, 82,* 483–491.

Konkolewicz, D., Hawkett, B. S., Gray-Weale, A., & Perrier, S. (2008). RAFT polymerization kinetics: Combination of apparently conflicting models. *Macromolecules, 41,* 6400–6412.

Monteiro, M. J., & De Brouwer, H. (2001). Intermediate radical termination as the mechanism for retardation in reversible addition-fragmentation chain transfer polymerization. *Macromolecules, 34,* 349–352.

Sarmoria, C., Asteasuain, M., & Brandolin, A. (2012). Prediction of molecular weight distributions in polymers using probability generating functions. *Canadian Journal of Chemical Engineering, 90,* 263–273.

Tobita, H. (2010). Modeling controlled/living radical polymerization kinetics: Bulk and miniemulsion. *Macromolecular Reaction Engineering, 4,* 643–662.

Wulkow, M., Busch, M., Davis, T. P., & Barner-Kowollik, C. (2004). Implementing the reversible addition-fragmentation chain transfer process in PREDICI. *Journal of Polymer Science Part A: Polymer Chemistry, 42,* 1441–1448.

Zapata-González, I., Saldívar-Guerra, E., & Ortiz-Cisneros, J. (2011). Full molecular weight distribution in RAFT polymerization. New mechanistic insight by direct integration of the equations. *Macromolecular Theory and Simulations, 20,* 370–388.

Zhang, M., & Ray, W. H. (2001). Modeling of "living" free-radical polymerization with RAFT chemistry. *Industrial & Engineering Chemistry Research, 40,* 4336–4352.